Supporting Information

Core-shell BaPP@BDO-Rh benzimidazole oligomer photocatalyst can effectively promote NADH regeneration and CO_2 conversion to fumarate

Guohua Li,[a,b,#] Zhiwen Lin,[b] Xiaodi Li,[b] Yahui Zhang,[b] Wenlong Zhu,[b]
Yusheng Shao,[b] Qiang Xue,b Qunfeng Fan,[b]
Tianwei Tana,[a,b,#] and Hui Cao,[b,#]

a Beijing Advance Center for Soft Matter Science and Engineering, Beijing University of Chemical Technology, Beijing, 100029 China.
b National Energy R&D Center for Biorefinery, Beijing Key Laboratory of Bioprocess, Beijing University of Chemical Technology. Beijing, 15th, Beisanhuan East Road, Beijing,100029，PR China.
Corresponding authors: Guohua Li (16622881217@163.com)，ORCID：0000-0002-7829-9941, Tianwei Tan (twtan@mail.buct.edu.cn), Hui Cao (caohui@mail.buct.edu.cn). 15 th, Beisanhuan East Road, Beijing, PR China.

Contents

1. Supplementary figures

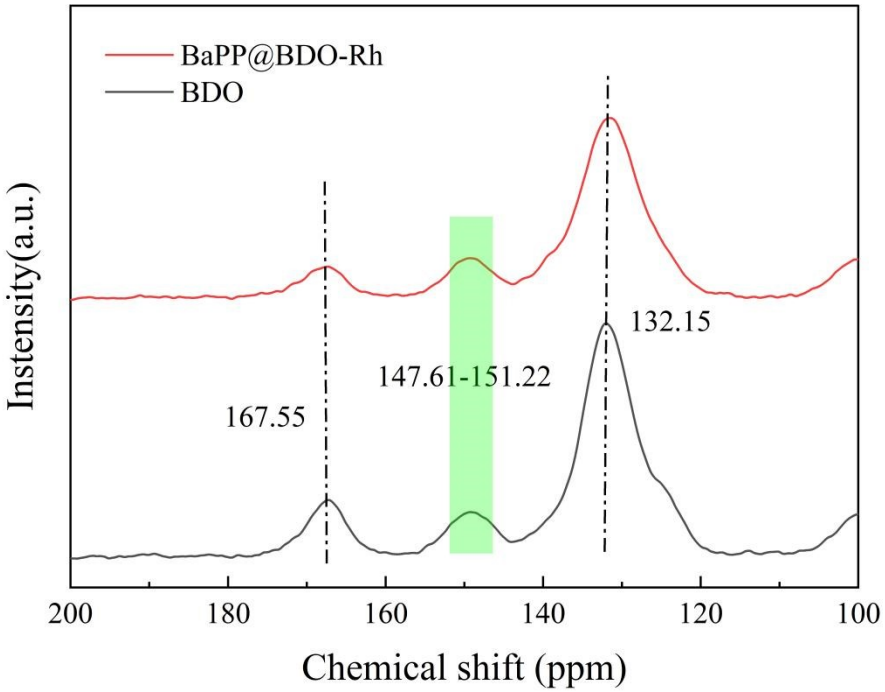

Fig. S1. The solid state 13C NMR spectra of BDO and BaPP@BDO-Rh.

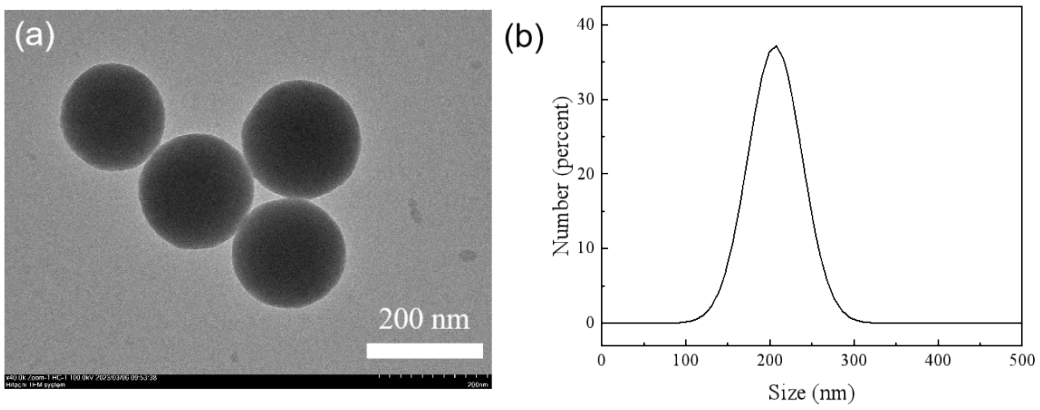

Fig. S2. (a) TEM images of nano-$BaSO_4$, (b) Particle size distribution of nano-$BaSO_4$. Particle size is obtained by testing the light scattering particle size instrument (Marvin, ZS-90).

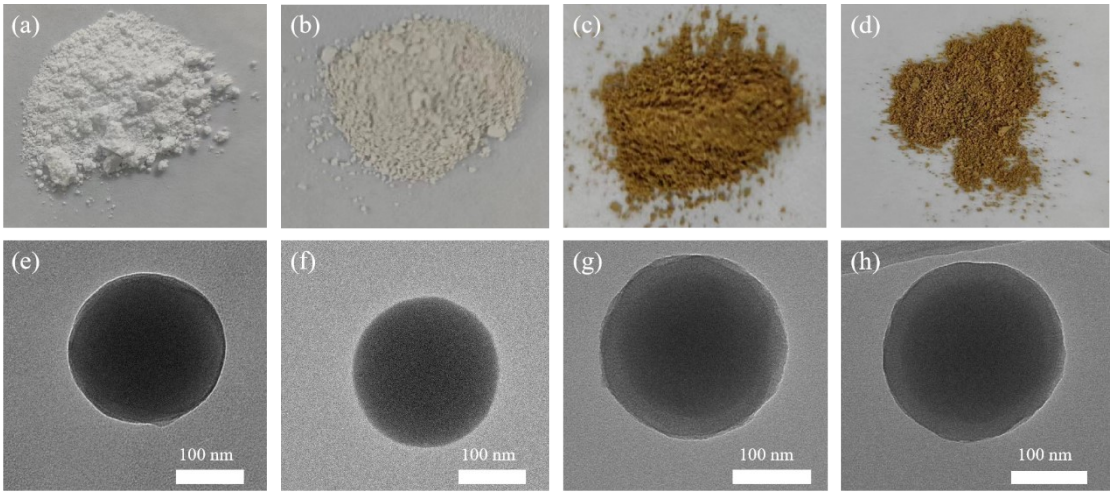

Fig. S3. (a-d) Optical images of (a) $BaSO_4$, (b) BaPP, (c) BaPP@BDO and (d) BaPP@BDO-Rh. (e-h) TEM images of (e) $BaSO_4$, (f) BaPP, (g) BaPP@BDO and (h) BaPP@BDO-Rh. BaPP@BDO and BaPP@BDO-Rh appear as bright yellow hydrogels in aqueous solution and as earthy-yellow powders when dried.

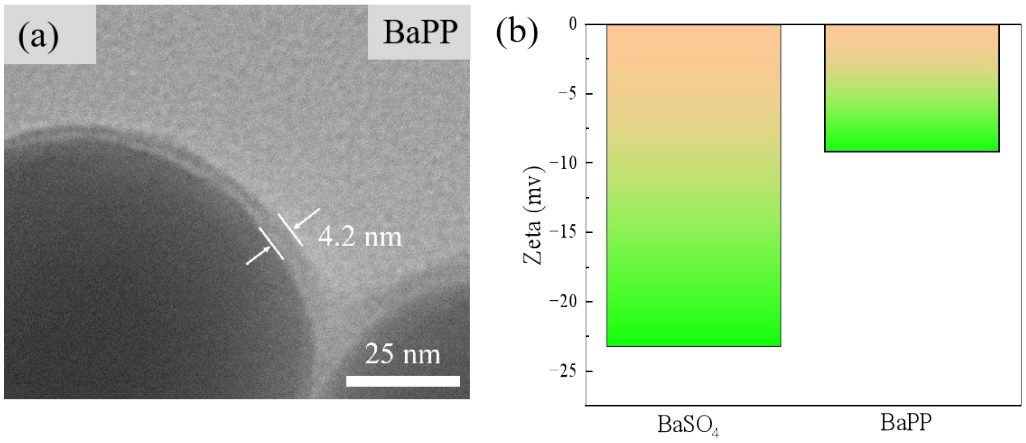

Fig. S4. (a) High-resolution TEM image of BaPP. (b) Zeta potential of $BaSO_4$ and BaPP.

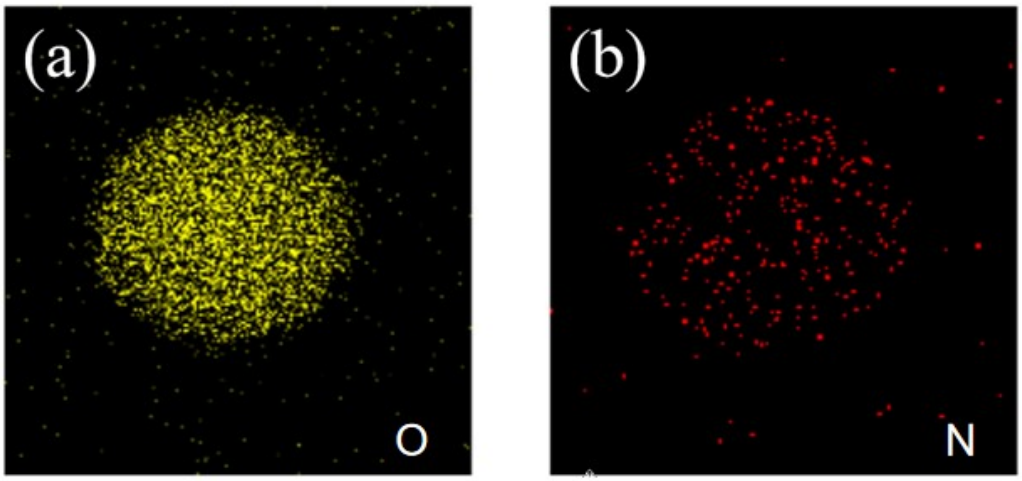

Fig. S5. (a) O and (b) N element mappings of BaPP@BDO-Rh.

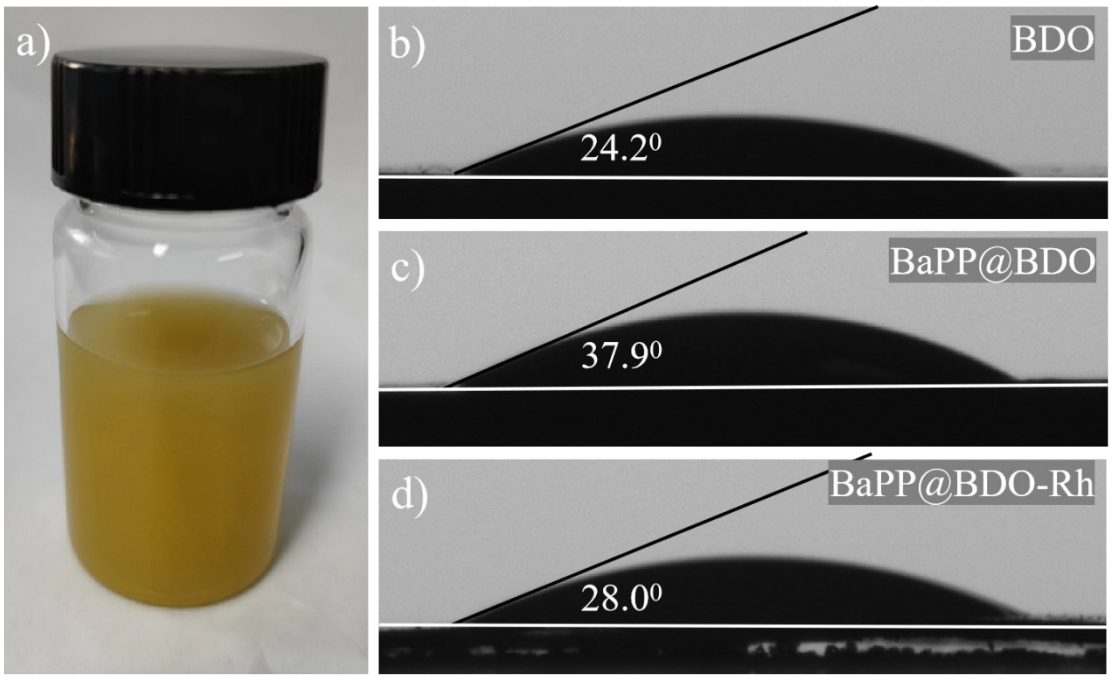

Fig. S6. a) Macroscopic image of BaPP@BDO-Rh in aqueous solution. Water contact angle test of b) BDO, c) BaPP@BDO and d) BaPP@BDO-Rh.

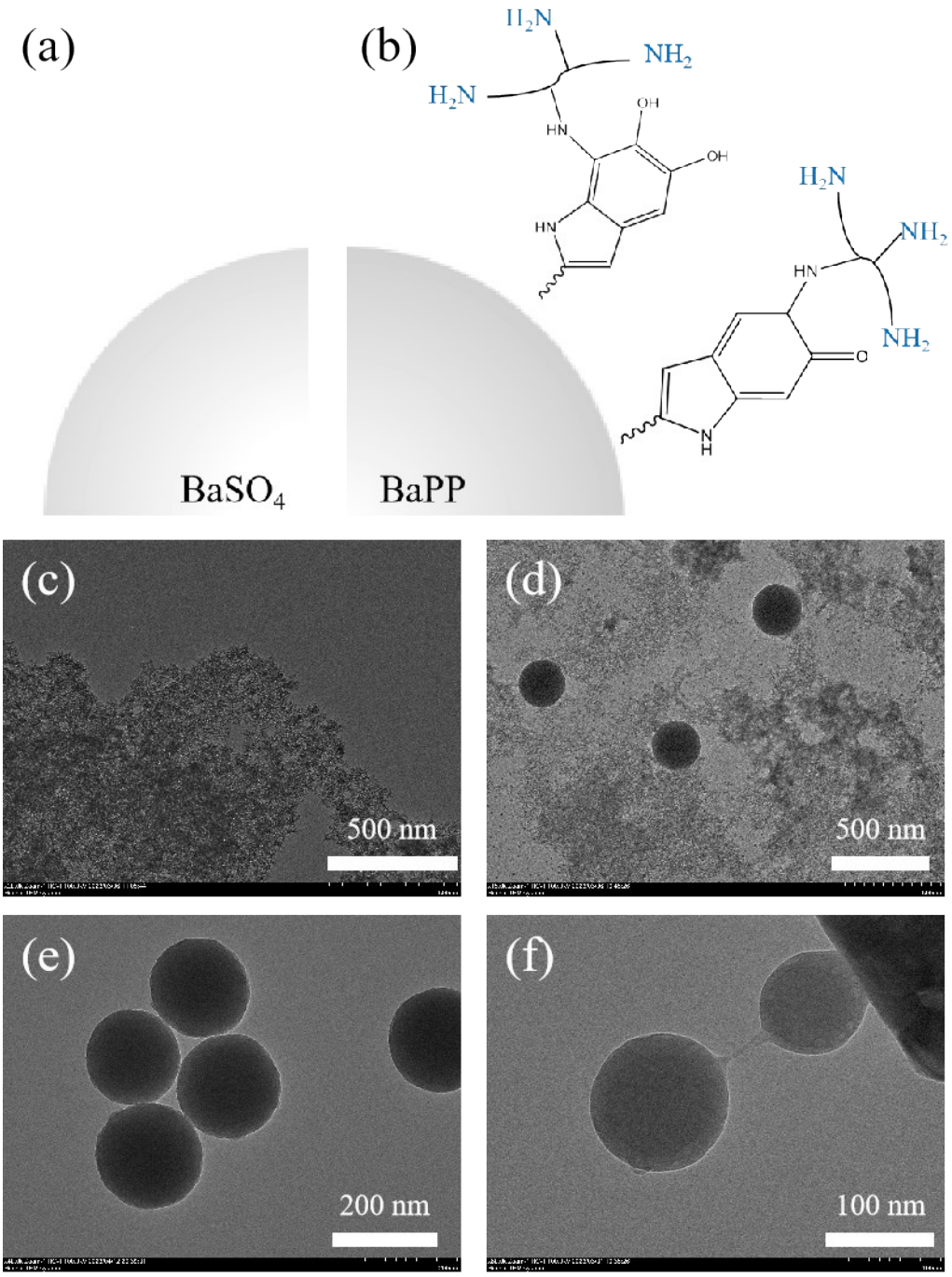

Fig. S7. The possible surface molecular structures of (a) $BaSO_4$ and (b) BaPP. (c-e) TEM images of (c) BDO, (d) $BaSO_4$/ BDO and (e,f) BaPP@BDO. By comparison, it is found that $BaSO_4$ without PEI/PDA modification is separated from BDO. Only PEI/PDA modified $BaSO_4$ and BDO can form core-shell structure.

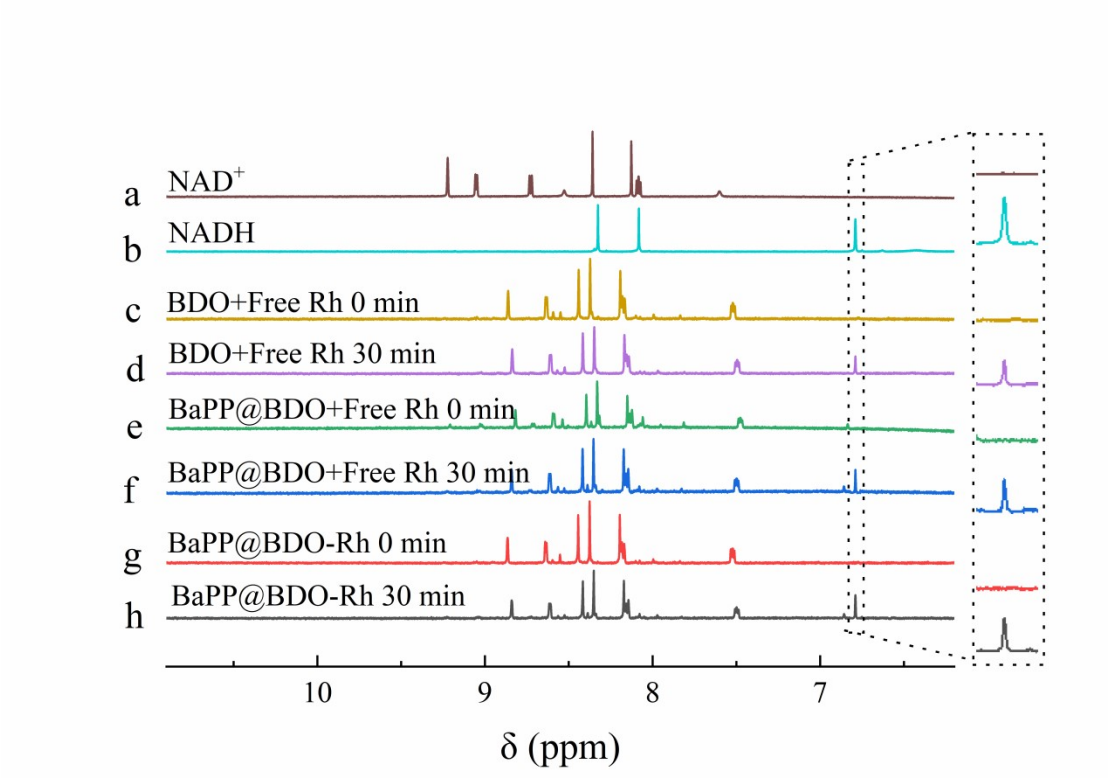

Fig. S8. ^{1}H NMR spectra of NAD^{+} (a) in D_2O, NADH (b) in D_2O, NADH regeneration system containing BDO+Free Rh (c,d), BaPP@BDO+Free Rh (e,f) and BaPP@BDO-Rh (g,h) before and after irradiated at xenon lamp. These peaks belonged to the hydrogen atoms on the pyridine ring after NAD^{+} was added to the reaction system. This phenomenon is thought to be caused by solvation effect.[1] Interestingly, no shift was observed in the characteristic peaks of NADH. By comparing the lines c and d, e and f, and g and h, the characteristic peak at 6.79 ppm validated the production of 1,4-NADH after illumination. Due to the limitation of detection signal, no signal of side-product was detected.

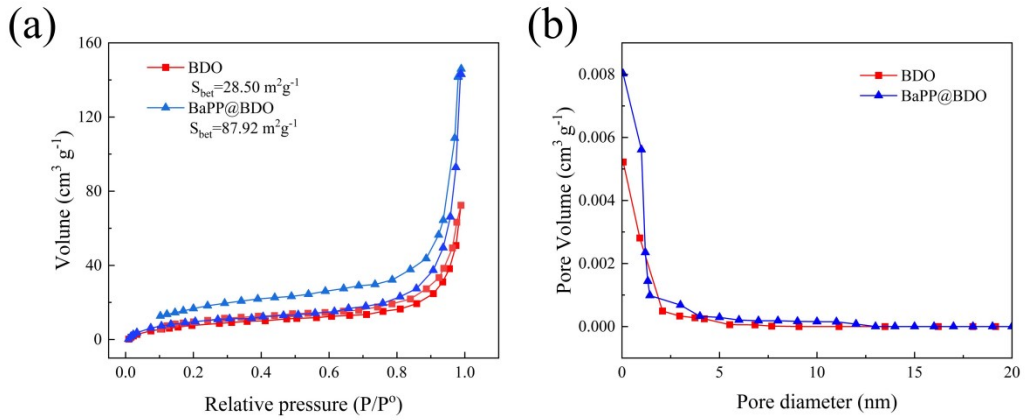

Fig. S9. (a) N_2 adsorption-desorption isotherms and (b) pore size distribution curves of BDO and BaPP@BDO.

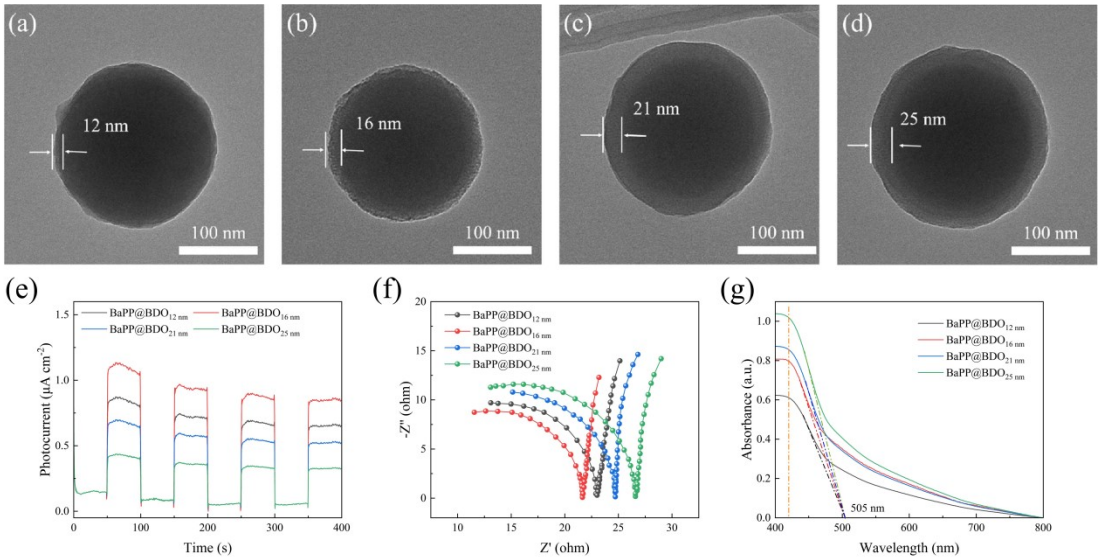

Fig. S10. (a-d) TEM images of (a) BaPP@BDO-$Rh_{12\ nm}$, (b) BaPP@BDO-$Rh_{16\ nm}$, (c) BaPP@ BDO-$Rh_{21\ nm}$ and (d) BaPP@BDO-$Rh_{25\ nm}$. (e) Photocurrent responses , (f) EIS Nyquist plots and UV−vis diffuse reflectance spectra of BaPP@BDO-$Rh_{12\ nm}$, BaPP@BDO-$Rh_{16\ nm}$, BaPP@BDO-$Rh_{21\ nm}$ and BaPP@BDO-$Rh_{25\ nm}$.

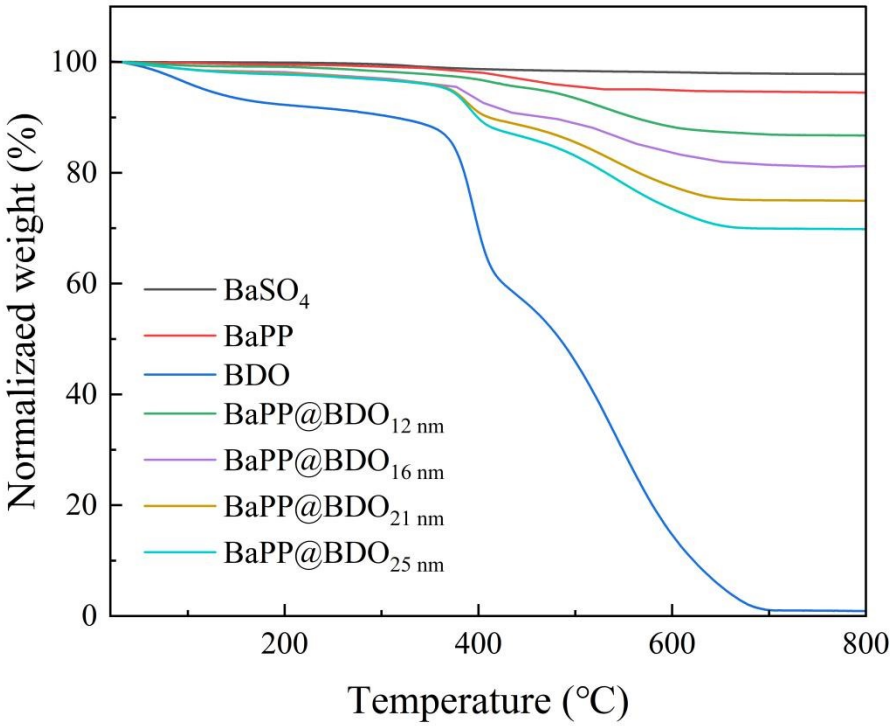

90

91 **Fig. S11.** Thermogravimetric analysis (TGA) profile of $BaSO_4$, BaPP,

92 BDO, BaPP@BDO $_{12\ nm}$, BaPP@BDO $_{16\ nm}$, BaPP@BDO $_{21\ nm}$ and

93 BaPP@BDO $_{25\ nm}$.

94

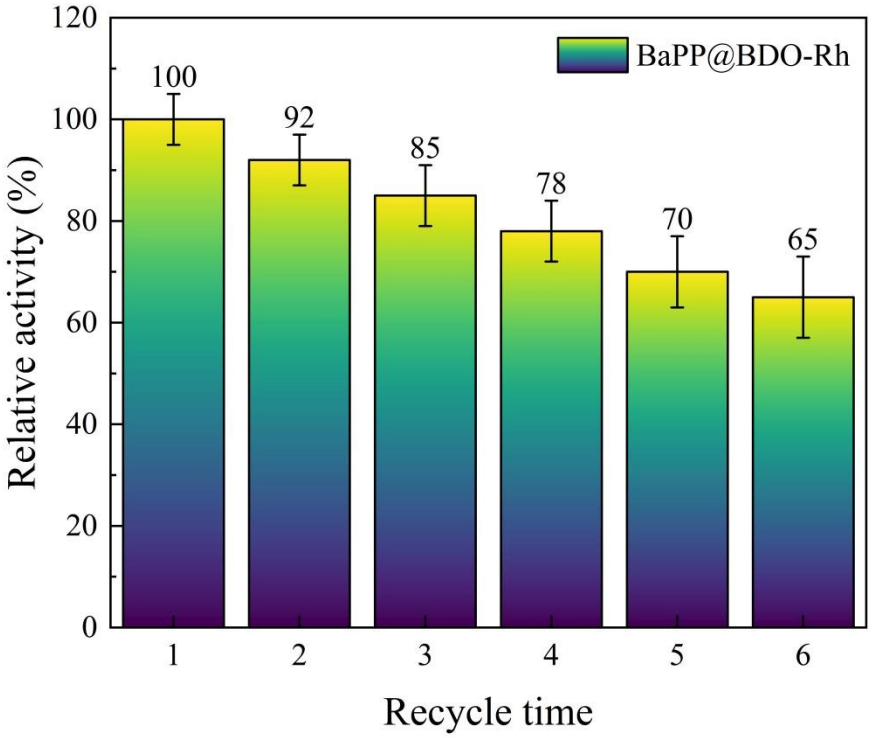

Fig. S12. Recycling stability of BaPP@BDO-Rh. The recycle stability of the catalytic system was evaluated by recovering the photocatalysts from the catalytic system by centrifugation (8000 rpm), and then, after washing three times, redispersing them into a new reaction solution for the next cycle.

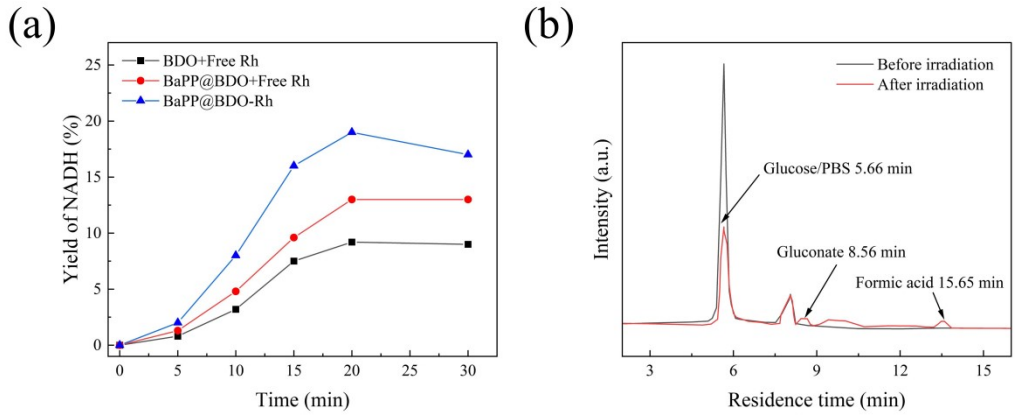

101

102 **Fig. S13. (**a) Yield of NADH as a fucntion of reaction time, (b) HPLC

103 analysis of the reaction solution before/after the reaction. Reaction

104 conditions: [photocatalyst] = 1 g L^{-1}; [Glucose/PBS] = 1000/100 mM ,

105 pH = 8.5; [NAD^+] = 1 mM; [free Rh] = 0.0188 mM; volume = 3 mL.

106

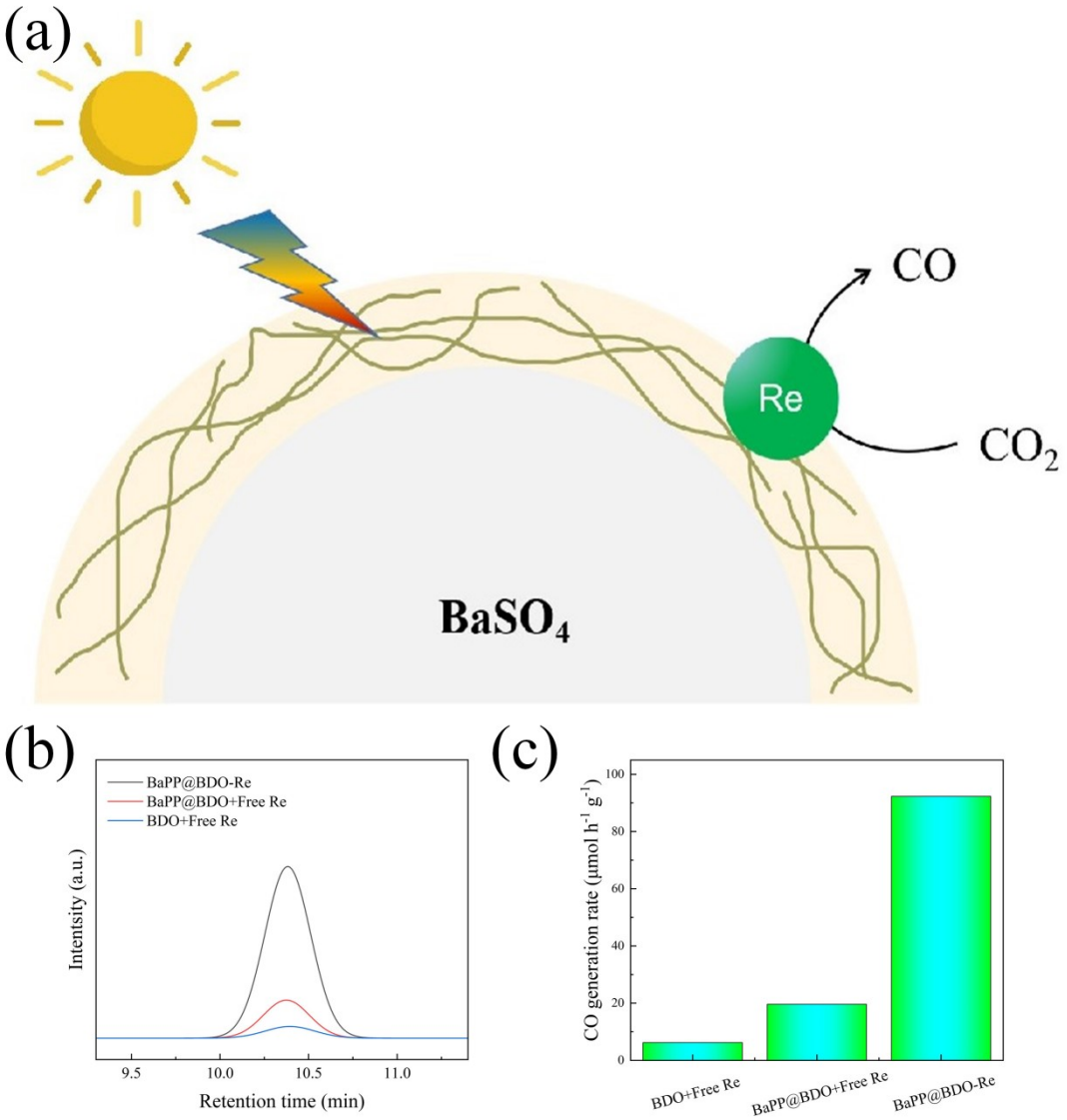

107

108 **Fig. S14.** Scheme of (a) BaPP@BDO-Re for photocatalytic CO_2

109 reduction. (b)Photocatalytic CO_2 reduction by BDO with free Re,

110 BaPP@BDO with free Re and BaPP@BDO-Re under 420 nm excitation

111 detected by gas chromatography and (c) calculated CO evolution rate.

112 Reaction conditions: photocatalyst (0.6 mg) was dispersed in 6 mL of

113 CH_3CN, and 0.4 mL of TEOA in 20 mL septum-sealed glass vials.

114

115

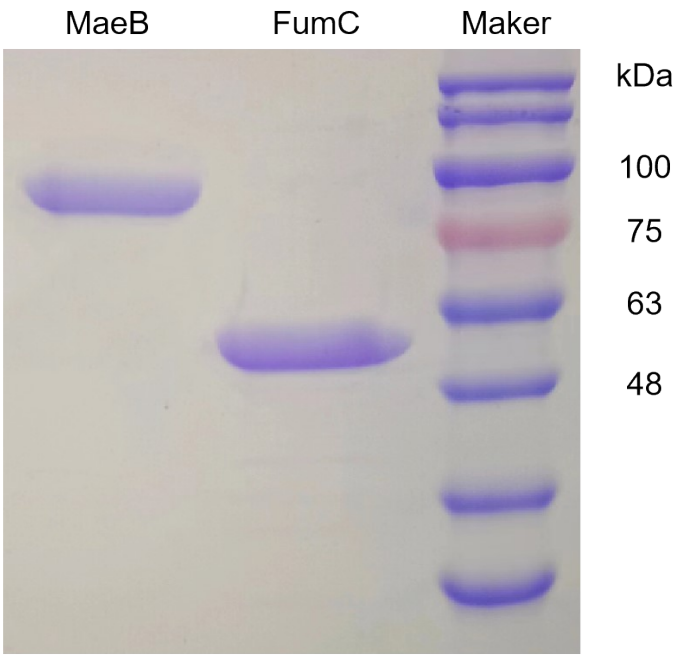

116

117 **Fig. S15.** SDS-PAGE analysis of the recombinant enzymes. Malate

118 dehydrogenase (MaeB);Fumarate hydrase (FumC).

119

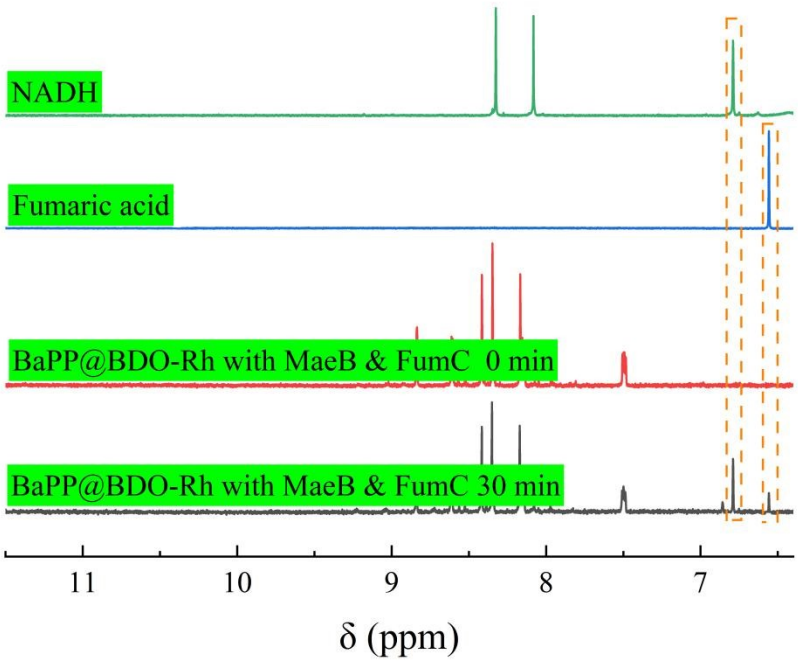

120

121 **Fig. S16.** ^{1}H NMR spectra of NADH and fumarate in a photoenzyme

122 catalyzed system.

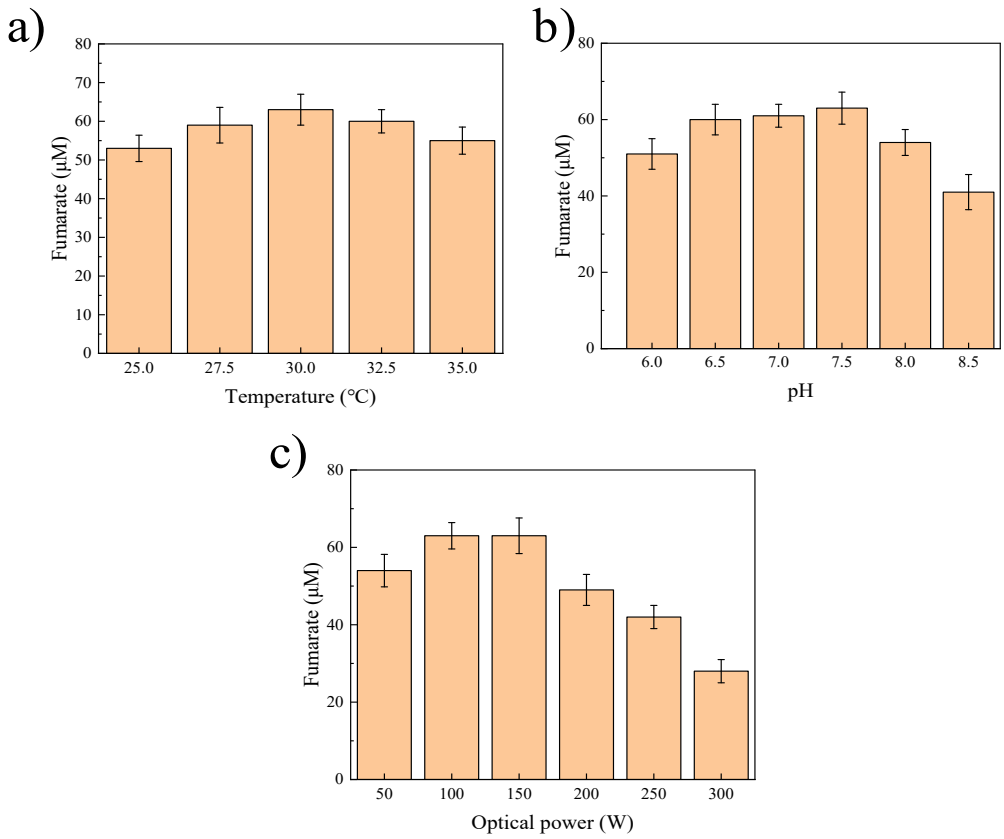

123

124 **Fig. S17.** Effect of temperature (a), pH (b) and optical power (c) on

125 photoenzyme-catalyzed synthesis of fumarate.

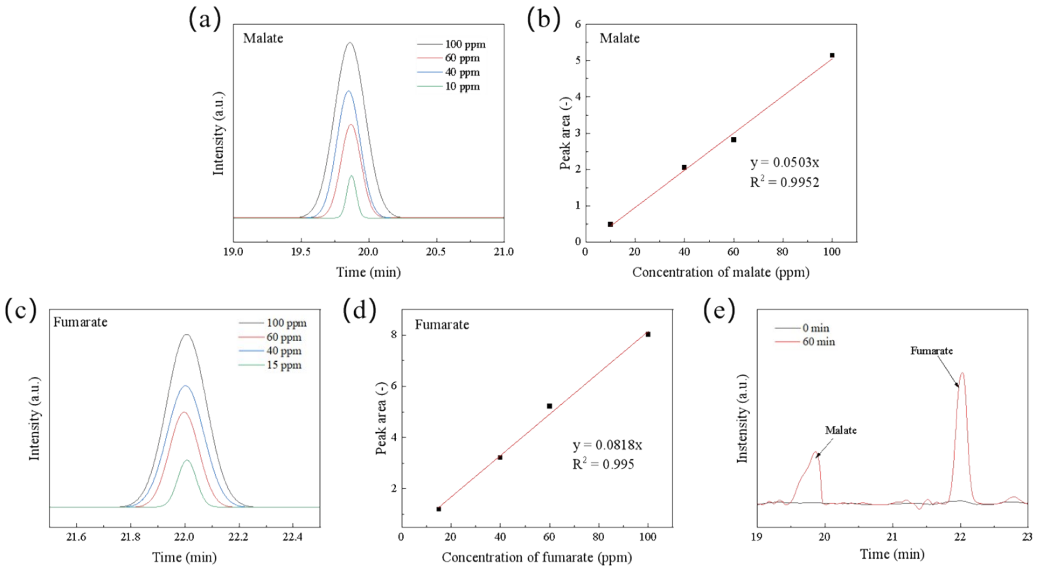

126

127 **Fig. S18.** (a) Ion chromatogram of standard malate at different

128 concentrations. (b) Relationship between the malate concentration and the

129 detection peak area. (c) Ion chromatogram of standard fumarate at

130 different concentrations. (b) Relationship between the fumarate

131 concentration and the detection peak area. (e) Ion chromatograms of

132 photoenzyme reaction for 0 min and 60 min.

133

134

135

136

2. Supplementary tables

Table S1. Parameters of time-resolved transient PL of BaPP@BDO and BaPP@BDO-Rh. After calculating[2] the parameters in Table S1, the fluorescence lifetimes of BaPP@BDO and BaPP@BDO-Rh can be calculated as 1.54 ns and 0.86 ns.

Photocatalyst	τ_1	τ_2	B_1	B_2
BaPP@BDO-Rh	0.4244	1.9088	0.054	0.005
BaPP@BDO	0.4265	1.9008	0.0057	0.004

142 **Table S2** The photocatalytic regeneration performance of NADH by

143 different photocatalysts.

Photocatalyst	Mediator	Reaction equilibrium time (min)	Yield (%)	TOF (h^{-1})
BaPP@BDO-Rh (Our study)	Rh	8	43.5	131.16
PCN@TA/PEI-Rh[3]	Rh	20	37.8	70.82
SiPP@CPNL-Rh[2]	Rh	28	39.6	44.8
GCN@M/TiO_2[4]	Rh	20	58	42.67
Co1/C_3N_4[5]	Rh	10	98	33.01
Rh-NU-1006[6]	Rh	120	28	20.69
TM@HOF-101[7]	Rh[a]	40	74.5	6.36
DBTS-CMP_1[8]	Rh	45	84	3.75
ACN[9]	Rh	60	62.3	3.36

ATCN-DSCN [10]	Rh	15	74	2.95
TCPP/SiO_2/Rh HNPs[11]	Rh	180	75	1.67
CTF[12]	Rh	120	75.9	0.76
AM/M/BP HNSs[13]	Rh	180	89	0.5

144 [a] Rh is $[Cp^*Rh(bpy)H_2O]^2$

Table S3. Reactions catalyzed by enzymes and BaPP@BDO-Rh in this system.

Enzyme	Reaction
Malate dehydrogenase (MaeB)	$NADH + Pyruvate + CO_2 \rightarrow Malate + NAD^+ + H^+ + 2e^{-1}$
Fumarate hydrase (FumC)	$Malate \rightarrow Fumarate + H_2O$
BaPP@BDO-Rh	$NAD^+ + H^+ + 2e^{-1} \rightarrow NADH$
Total reaction	$Pyruvate + CO_2 \rightarrow Malate + H_2O$

Table S4. Information about enzymes used in this study.

Enzyme	EC number	Soure	Sp. Act ($U\ mg^{-1}$)
Malate dehydrogenase (MaeB)	1.1.1.40	*E.coli*	1.76
Fumarate hydrase (FumC)	4.2.1.2	*R. capsulata*	6.29

3. References

1. J. Qiu, B. Song, X. Li and A. Cozzolino, *Physical Chemistry Chemical Physics*, 2018, **20**, 46-50.
2. S. Li, Y. Cheng, Y. Chen, J. Li, Y. Sun, J. Shi and Z. Jiang, *Applied Catalysis B: Environmental*, 2022, **317**, 121772.
3. Y. Cheng, J. Shi, Y. Wu, X. Wang, Y. Sun, Z. Cai, Y. Chen and Z. Jiang, *Research (Wash D C)*, 2021, **2021**, 8175709.
4. S. Zhang, Y. Zhang, Y. Chen, D. Yang, S. Li, Y. Wu, Y. Sun, Y. Cheng, J. Shi and Z. Jiang, *ACS Catalysis*, 2020, **11**, 476-483.
5. W. Liu, W. Hu, L. Yang and J. Liu, *Nano Energy*, 2020, **73**, 104750.
6. Y. Chen, P. Li, J. Zhou, C. T. Buru, L. Dordevic, P. Li, X. Zhang, M. M. Cetin, J. F. Stoddart, S. I. Stupp, M. R. Wasielewski and O. K. Farha, *J Am Chem Soc*, 2020, **142**, 1768-1773.
7. G. Li, X. Lv, W. Ji, Y. Zhou, Z. Lin, H. Cao and T. Tan, *Journal of Materials Chemistry C*, 2023, **11**, 7411-7418.
8. F. Lan, Q. Wang, H. Chen, Y. Chen, Y. Zhang, B. Huang, H. Liu, J. Liu and R. Li, *ACS Catalysis*, 2020, **10**, 12976-12986.
9. E. J. Son, Y. W. Lee, J. W. Ko and C. B. Park, *ACS Sustainable Chemistry & Engineering*, 2018, **7**, 2545-2552.
10. J. Meng, Y. Tian, C. Li, X. Lin, Z. Wang, L. Sun, Y. Zhou, J. Li, N. Yang, Y. Zong, F. Li, Y. Cao and H. Song, *Catalysis Science &*

Technology, 2019, **9**, 1911-1921.

11. X. Ji, J. Wang, L. Mei, W. Tao, A. Barrett, Z. Su, S. Wang, G. Ma, J. Shi and S. Zhang, *Advanced Functional Materials*, 2018, **28**, 1705083.
12. R. K. Yadav, A. Kumar, N.-J. Park, K.-J. Kong and J.-O. Baeg, *Journal of Materials Chemistry A*, 2016, **4**, 9413-9418.
13. X. Ji, Y. Kang, T. Fan, Q. Xiong, S. Zhang, W. Tao and H. Zhang, *Journal of Materials Chemistry A*, 2020, **8**, 323-333.